

Enhanced Device Performance Through Optimization of Acceptor Layer Thickness Relative to Exciton Diffusion Length and Ionization Energy Offset in Bilayer Organic Solar Cells

Yexiao Huang^{1†}, Abdul Azeez^{1†}, Jingjing Zhao², Zhenmin Zhao¹, Muneendra Dassanagari¹, Frédéric Laquai³⁺, Zhipeng Kan^{2*}, and Safakath Karuthedath^{1*}

¹Institute of Materials Research, Tsinghua Shenzhen International Graduate School, Tsinghua University, Shenzhen, 518055 China.

²Center on Nanoenergy Research, Guangxi Colleges and Universities Key Laboratory of Blue Energy and Systems Integration, Institute of Science and Technology for Carbon Peak & Neutrality, School of Physical Science & Technology, Guangxi University, Nanning 530004, China.

³King Abdullah University of Science and Technology (KAUST), KAUST Solar Center (KSC), Physical Sciences and Engineering Division (PSE), Material Science and Engineering Program (MSE), Thuwal 23955-6900, Kingdom of Saudi Arabia

[†]Present Address: Department of Chemistry, Ludwig-Maximilians-Universität München, Butenandtstraße 5-13 (E), D-81377 München, Germany

*Email: kanzhipeng@gxu.edu.cn, safakath@sz.tsinghua.edu.cn

Contents

1. Device Fabrication	3
2. Atomic Force Microscopy (AFM) Measurement	4
3. Acceptor Layer Thickness Optimization Results.....	5
4. EQE characteristics	7
5. Thin Film Characterization	7
6. Transient Photocurrent (TPC) and Transient Photovoltage (TPV)	10
7. Carrier extraction by linearly increasing voltage (CELIV).....	11

1. Device Fabrication

The architecture of b-OSCs is ITO/Donor polymer/COi8DFIC/PDIN/Ag. A thin layer (ca. 30 nm) of PEDOT:PSS (Clevios AL4083) was first spin-coated on the pre-cleaned ITO-coated glass substrates at 4000 rpm and baked at 150 °C for 15 min under ambient conditions. Subsequently, the donor and acceptor layers were prepared separately. The PTB7-Th (PBDB-T, PBDB-T-2F) solutions were prepared in CF at 8 mg/mL whereas COi8DFIC solutions were prepared in DCM at 10 mg/ml, the acceptor thickness was controlled by varying the concentration of the COi8DFIC solution. PDIN in carbinol with 0.3% acetic acid at 2 mg/mL was then spin-coated on the active layer at 4000 rpm. At the final stage, the substrates were pumped down in a high vacuum, and Ag (100 nm) was thermally evaporated onto the active layer.

Table S1. Thickness of PTB7-Th/COI8DFIC device

Materials		Thickness (nm)	
PTB7-Th (8mg/ml)		55	
Materials		<u>PTB7-Th/COI8DFIC</u>	<u>COI8DFIC</u>
PTB7-Th/COI8DFIC	(8mg/ml 6mg/ml)	95	32
PTB7-Th/COI8DFIC	(8mg/ml 8mg/ml)	102	40
PTB7-Th/COI8DFIC	(8mg/ml 10mg/ml)	108	50
PTB7-Th/COI8DFIC	(8mg/ml 12mg/ml)	122	59
PTB7-Th/COI8DFIC	(8mg/ml 14mg/ml)	153	83

Table S2. The thickness of the PBDB-T/COI8DFIC device

Materials		Thickness (nm)	
PBDB-T (8mg/ml)		60	
Materials		<u>PBDB-T/COI8DFIC</u>	<u>COI8DFIC</u>
PBDB-T/COI8DFIC	(8mg/ml 6mg/ml)	102	32
PBDB-T/COI8DFIC	(8mg/ml 8mg/ml)	122	40
PBDB-T/COI8DFIC	(8mg/ml 10mg/ml)	131	50
PBDB-T/COI8DFIC	(8mg/ml 12mg/ml)	151	59
PBDB-T/COI8DFIC	(8mg/ml 14mg/ml)	168	83

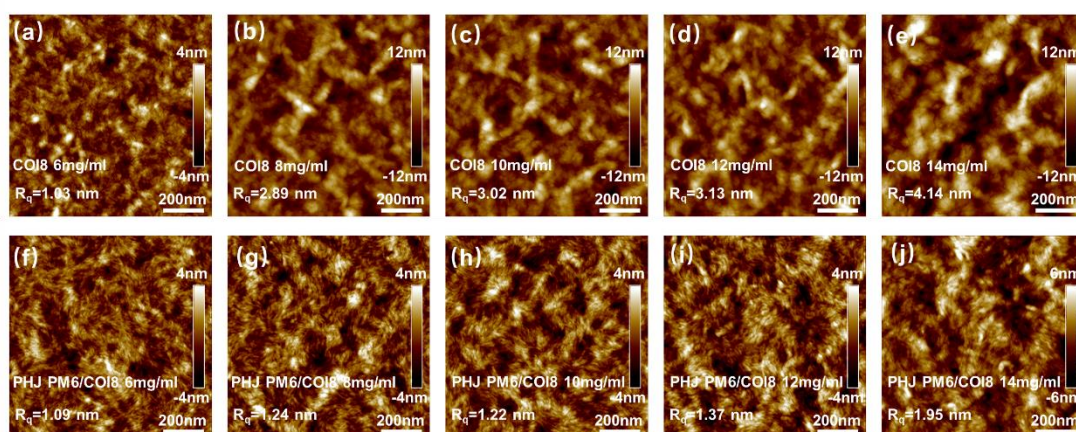
Table S3. The Thickness of PBDB-T-2F/COi8DFIC device

Materials		Thickness
PBDB-T-2F (8mg/ml)		55
Materials		PBDB-T-2F/COi8DFIC
		COi8DFIC
PBDB-T-2F/COi8DFIC	(8mg/ml 6mg/ml)	86
PBDB-T-2F/COi8DFIC	(8mg/ml 8mg/ml)	100
PBDB-T-2F/COi8DFIC	(8mg/ml 10mg/ml)	122
PBDB-T-2F/COi8DFIC	(8mg/ml 12mg/ml)	145
PBDB-T-2F/COi8DFIC	(8mg/ml 14mg/ml)	165

Thickness Measurement: The thickness of the films was measured using a surface profilometer (KLA Corporation D-100 Stylus Profilometer). To ensure accuracy, the thickness was determined as an average of measurements taken at three different positions on each film.

2. Atomic Force Microscopy (AFM) Measurement

A Dimension Icon atomic force microscope (AFM) from Bruker was used to image the active layers in tapping mode. The film preparation process is consistent with



that described in Section 1.

Figure S1. AFM height images of (a-e) different thicknesses of the COi8DFIC films, and (f-j) the corresponding PBDB-T-2F/COi8DFIC films.

3. Acceptor Layer Thickness Optimization Results

The current density-voltage (J - V) characteristics of b-OSCs were measured using a Keithley 2400 source meter in the glove box under AM 1.5G (100 mW cm⁻²) illumination conditions using an Enlitech solar simulator. The external quantum efficiency (EQE) spectra were measured using a Solar Cell Spectral Response Measurement System QE-R3011 (Enlitech Co., Ltd.). The light intensity at each wavelength was calibrated using a standard monocrystalline Si photovoltaic cell. The transient photocurrent (TPC) and transient photovoltage (TPV) measurements were performed using the PAIOS electro-optical characterization module (fluxim, Switzerland).

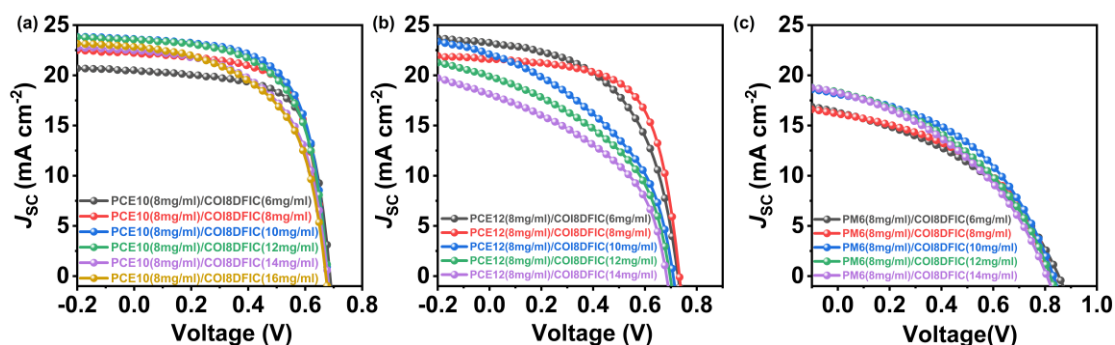


Figure S2. Typical J - V characteristic curves of different bilayer organic solar cells optimized in the study (Table S4 summarizes the result). Note that the donor polymers are well known by their alternate names such as PTB7-Th (PCE10), PBDB-T (PCE12), and PBDB-T-2F (PM6) respectively.

Table S4. Photovoltaic parameters of the optimized PTB7-Th/COi8DFIC OSCs under simulated AM1.5G illumination (100 mW cm⁻²).

Donor	Acceptor	Active Layer	V_{OC} (V)	PCE ^a (%)	FF (%)	J_{SC} (mA/cm ²)
8mg/ml	6mg/ml	PTB7-	0.684	9.70	67.90	20.90
		Th/COi8DFIC	± 0.002	± 0.10	± 0.11	± 0.20
8mg/ml	8mg/ml	PTB7-	0.679	11.42	65.91	25.53
		Th/COi8DFIC	± 0.003	± 0.45	± 1.54	± 0.74
8mg/ml	10mg/ml	PTB7-	0.680	10.03	63.14	23.36
		Th/COi8DFIC	± 0.004	± 0.27	± 1.04	± 0.42
8mg/ml	12mg/ml	PTB7-	0.676	9.73	61.55	23.39
		Th/COi8DFIC	± 0.003	± 0.29	± 2.02	± 0.22
8mg/ml	14mg/ml	PTB7-	0.675	8.66	58.21	22.06
		Th/COi8DFIC	± 0.004	± 0.15	± 1.45	± 0.52

8mg/ml	16mg/ml	PTB7- Th/COi8DFIC	0.671 ± 0.002	8.59 ± 0.08	56.48 ± 0.39	22.68 ± 0.18
--------	---------	----------------------	------------------	----------------	-----------------	-----------------

Table S5. *J-V* Photovoltaic parameters of the optimized PBDB-T/COi8DFIC OSCs under simulated AM1.5G illumination (100 mW cm⁻²).

Donor	Acceptor	Active Layer	V _{oc} (V)	PCE ^a (%)	FF (%)	J _{sc} (mA/cm ²)
8mg/ml	6mg/ml	PBDB-T/COi8DFIC	0.721 ± 0.004	9.14 ± 0.14	52.15 ± 1.18	24.32 ± 0.73
8mg/ml	8mg/ml	PBDB-T/COi8DFIC	0.730 ± 0.005	9.78 ± 0.36	60.52 ± 4.59	22.17 ± 1.12
8mg/ml	10mg/ml	PBDB-T/COi8DFIC	0.713 ± 0.003	6.69 ± 0.13	42.90 ± 0.53	21.87 ± 0.33
8mg/ml	12mg/ml	PBDB-T/COi8DFIC	0.700 ± 0.004	5.47 ± 0.43	42.4 1.96	18.39 ± 0.84
8mg/ml	14mg/ml	PBDB-T/COi8DFIC	0.699 ± 0.008	5.38 ± 0.17	42.48 ± 1.61	18.14 ± 0.41

Table S6. Photovoltaic parameters of the optimized PBDB-T-2F/COi8DFIC OSCs under simulated AM1.5G illumination (100 mW cm⁻²).

Donor	Acceptor	Active Layer	V _{oc} (V)	PCE ^a (%)	FF (%)	J _{sc} (mA/cm ²)
8mg/ml	6mg/ml	PBDB-T-2F/COi8DFIC	0.853 ± 0.002	5.71 ± 0.03	41.08 ± 0.23	16.29 ± 0.10
8mg/ml	8mg/ml	PBDB-T-2F/COi8DFIC	0.827 ± 0.005	5.84 ± 0.14	44.13 ± 0.91	16.00 ± 0.14
8mg/ml	10mg/ml	PBDB-T-2F/COi8DFIC	0.835 ± 0.005	6.57 ± 0.15	44.11 ± 0.64	17.82 ± 0.33
8mg/ml	12mg/ml	PBDB-T-2F/COi8DFIC	0.813 ± 0.005	5.97 ± 0.19	41.07 ± 0.62	17.87 ± 0.52
8mg/ml	14mg/ml	PBDB-T-2F/COi8DFIC	0.805 ± 0.001	5.64 ± 0.12	39.29 ± 0.38	17.84 ± 0.25

4. EQE characteristics

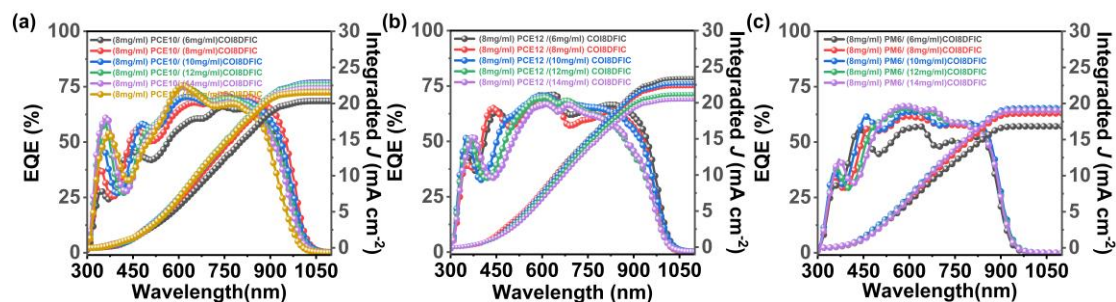


Figure S3. EQE characteristic curves of different bilayer organic solar cells.

Table S7 Integrated J_{SC} of PHJ devices.

Active Layer	integrated J_{SC} ^a					
	6mg/ml	8mg/ml	10mg/ml	12mg/ml	14mg/ml	16mg/ml
PTB7-Th/COi8DFIC	20.35	22.91	22.85	22.52	22.06	21.54
PBDB-T/COi8DFIC	23.40	22.31	22.69	21.18	20.46	/
PBDB-T-2F/COi8DFIC	16.84	18.62	19.34	19.10	19.06	/

^a Integrated J_{SC} in different acceptor thickness

5. Thin Film Characterization

TRPL measurements were performed on films spin-coated onto quartz substrates using the output of a Mode-locked Ti:Sa (Chameleon Ultra I from Coherent) fs laser operating at 80 MHz repetition rate, at 725 nm. An optical telescope (consisting of two plano-convex lenses) collected the PL of the samples, focused on the slit of a spectrograph (Princeton Instrument Spectra Pro SP2300), and detected with a Streak Camera (Hamamatsu C10910) system; a long pass filter (750 nm) was used. The excitation fluences used were between 0.3 to 3 nJ/cm² where no fluence dependence was observed for these materials. The data were acquired in time-correlated single photon counting mode using the Streak Camera software (HPDTA) and exported to Origin 2021 for further analysis.

Transient absorption (TA) spectroscopy was carried out using a custom pump-probe setup. The output of a titanium:sapphire amplifier (Coherent LEGEND DUO,

4.5 mJ, 3 kHz, 100 fs) was split into three beams (2, 1, and 1.5 mJ). One of them was used to produce a white-light supercontinuum from 550 to 1700 nm by sending the 800 nm pulses through a sapphire (3 mm thick) crystal. The other two beams were used to pump two optical parametric amplifiers (OPA) separately (Light Conversion TOPAS Prime). TOPAS 1 generates tunable pump pulses, while TOPAS 2 generates signal (1300 nm) and idler (2000 nm) only. The pump-probe delay was adjusted by reducing the pump beam pathway between 5.12 and 2.6 m while the probe pathway length to the sample was kept constant at ≈ 5 m between the output of TOPAS 1 and the sample. The pump-probe path length was varied with a broadband retroreflector mounted on an automated mechanical delay stage (Newport linear stage IMS600CCHA controlled by a Newport XPS motion controller), thereby generating delays between pump and probe from -400 ps to 8 ns. The samples (films on quartz substrates) were kept under vacuum (10^{-6} mbar) during the measurements. The excitation wavelength used was 750 nm. The transmitted fraction of the white light was guided to a custom-made prism spectrograph (Entwicklungsbüro Stresing), where it was dispersed by a prism onto a 512-pixel complementary metal-oxide-semiconductor (CMOS) linear image sensor (Hamamatsu G11608- 512DA). The probe pulse repetition rate was 3 kHz, while the excitation pulses were directly generated at 1.5 kHz frequency, and the detector array was read out at 3 kHz. Adjacent diode readings corresponding to the transmission of the sample after excitation and in the absence of an excitation pulse were used to calculate $\Delta T/T$. Measurements were averaged over several thousand shots to obtain a good signal-to-noise ratio. The chirp induced by the transmissive optics was corrected with a custom MATLAB script. The delay at which the pump and probe arrive simultaneously on the sample (i.e., zero time) was determined from the point of the maximum positive slope of the TA signal rise for each wavelength.

In this work, we employed the exciton annihilation method to calculate the exciton diffusion length, providing validation for diffusion length measurements based on photocurrent. To further investigate, we utilized ultrafast transient absorption (TA) spectroscopy to measure the exciton lifetime as a function of excitation density. These measurements were performed on films without requiring an exciton quenching interface.

As the excitation flux increased, exciton annihilation was observed, leading to an accelerated exciton decay. The excitation flux range used here is from 1.1 to 16 $\mu\text{J cm}^{-2}$. The exciton decay can be globally fitted to the rate equation that considers both exciton annihilation and first-order exciton recombination ¹:

$$\frac{dn(t)}{dt} = \kappa n(t) - \frac{1}{2}\alpha n^2(t) \quad (1)$$

The solution is:

$$n(t) = \frac{n(0)e^{-\kappa t}}{1 + \frac{\alpha}{2\kappa}n(0)[1 - e^{-\kappa t}]} \quad (2)$$

Here, κ is the fluorescence decay rate constant in the absence of any annihilation, α is the rate constant for singlet-singlet bimolecular exciton annihilation, and $n(t)$ is the singlet exciton density as a function of time after laser excitation. The measurements require the preparation of two sets of films on a quartz glass substrate: (1) neat acceptor films to obtain the α value, and (2) a dilute acceptor in polystyrene films to extract κ (or the intrinsic exciton lifetime, $\tau = 1/\kappa$).

Generally, the exciton diffusion length is defined as the root mean squared value of the exciton diffusion distances. The thus defined diffusion length is deduced to be $L_D = \sqrt{2dD\tau}$, in which d is the dimensionality factor, D is the diffusion constant given by $D = \alpha/(8\pi R)$ (three-dimensional diffusion model), R is the annihilation radius of singlet excitons. The annihilation radius cannot be easily measured and generally assumed to be 1 nm ^[1-5]. For the three-dimensional diffusion, strictly speaking, the diffusion length should be $\sqrt{6D\tau}$. However, it is a common practice in literature (especially experimental works) to use $\sqrt{D\tau}$ to represent the diffusion length. Although the dimensionality factor is omitted, it is straightforward to calculate the diffusion length in the 2 or 3 dimensions by multiplying $\sqrt{D\tau}$ with 2 or $\sqrt{6}$, respectively. Moreover, for some cases, the 1-d diffusion length is more relevant than the 3-d one, such as the donor/acceptor bilayer system where only the exciton diffusion along the thickness direction contributes to the charge separation; or with finite

light penetration depth in thick films, the exciton distribution is inhomogeneous, and the exciton diffusion occurs predominantly along the exciton density gradient. Above all, the 1d exciton diffusion length equation can well describe the diffusion behavior in our experiments.³⁻⁵

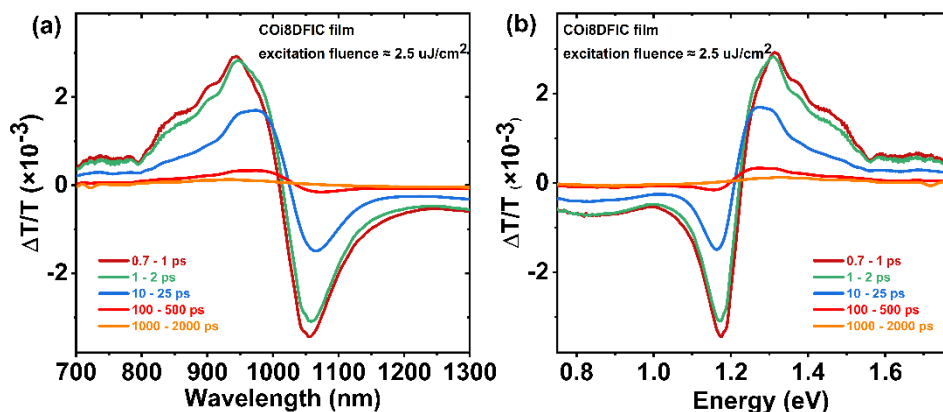


Figure S4. Typical transient absorption spectra of a neat COi8DFIC film used to estimate the exciton diffusion length. (a) Transient absorption spectra are plotted as a function of wavelength and (b) transient absorption spectra are plotted as a function of energy.

6. Transient Photocurrent (TPC) and Transient Photovoltage (TPV)

The transient photocurrent (TPC) and transient photovoltage (TPV), measurements were conducted using the PAIOS electro-optical characterization module (Fluxim Co., Switzerland), integrated with the Setfos-Paios numerical simulation module. A global fitting approach was utilized to extract the device parameters.

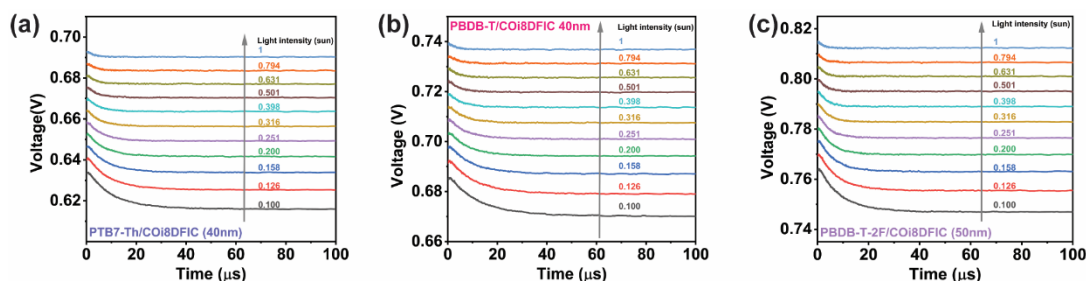


Figure S5. (a-c) Transient photovoltage decay profile of the PTB7-Th/COi8DFIC, PBDB-T/COi8DFIC, and PBDB-T-2F/COi8DFIC bilayer OSCs with measurement performed at different background light intensity levels indicated in the inset.

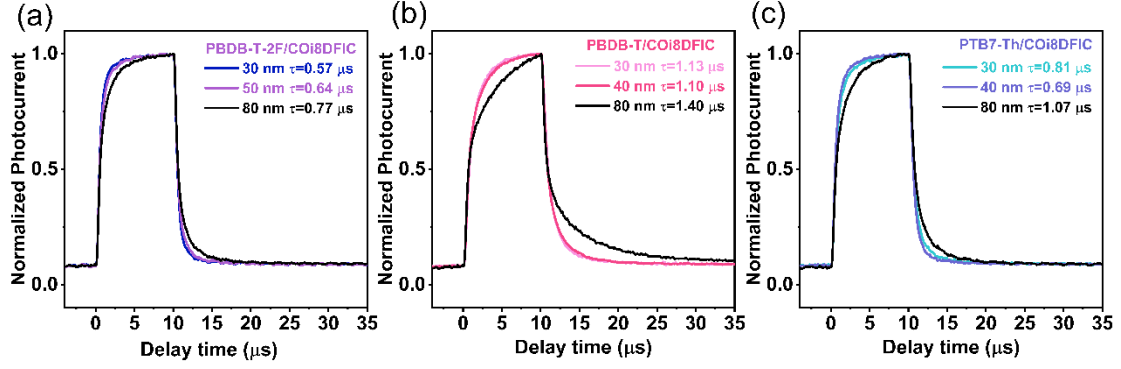


Figure S6. (a-c) Transient photocurrent profile of the PBDB-T-2F/COi8DFIC, PBDB-T/COi8DFIC, and PTB7-Th/COi8DFIC bilayer OSCs with different COi8DFIC thicknesses.

7. Carrier extraction by linearly increasing voltage (CELIV)

According to Mozer *et al.*'s recombination model, carrier density $n(t)$ over time can be expressed as: ^[6-8]

$$n(t) = \frac{n_0}{1 + \left(\frac{t}{\tau_b}\right)^\gamma} \quad (1)$$

where $n(t)$ is the charge density at time t , n_0 is the initial charge density, τ_b is the recombination lifetime, and γ is the dispersion parameter. The dispersion parameter $\gamma=1$ for trap-free non-dispersive bimolecular recombination and is <1 for dispersive bimolecular recombination.

In the dispersive bimolecular recombination, the decay of carrier density is given by:

$$\beta(t) = -\frac{dn(t)/dt}{n^2(t)} \quad (2)$$

where $n(t)$ is the carrier density and $\beta(t)$ is dispersive bimolecular recombination rate at a delay time t . Substituting **equation (1)**, the bimolecular recombination rate $\beta(t)$ can also be expressed as: ^[3]

$$\beta(t) = (1/\tau_b)\gamma n_0^{-1}(t/\tau_b)^{\gamma-1} \quad (3)$$

The resulting $\beta(t)$ can be calculated from the fitting parameters $n(0)$, τ_b and γ using **equation (3)**.

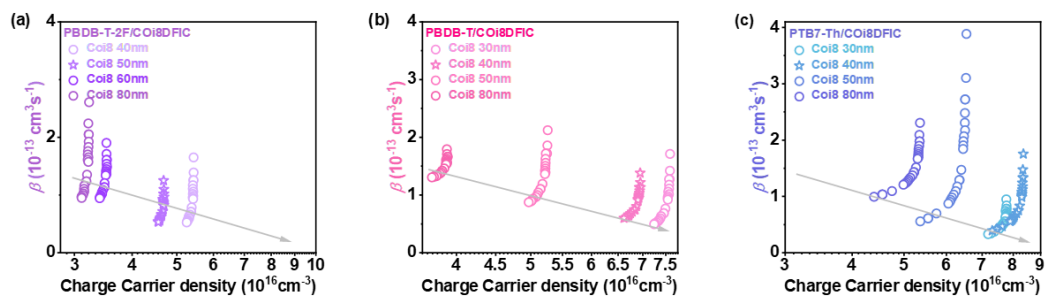


Figure S7. Bimolecular recombination rate versus charge carrier density obtained from the Photo-CELIV traces with varied delay times from 10 ns to 1 μ s in b-OSCs with different acceptor layer thicknesses (a) PBDB-T-2F/COi8DFIC, (b) PBDB-T/COi8DFIC, and (c) PTB7-Th/COi8DFIC respectively.

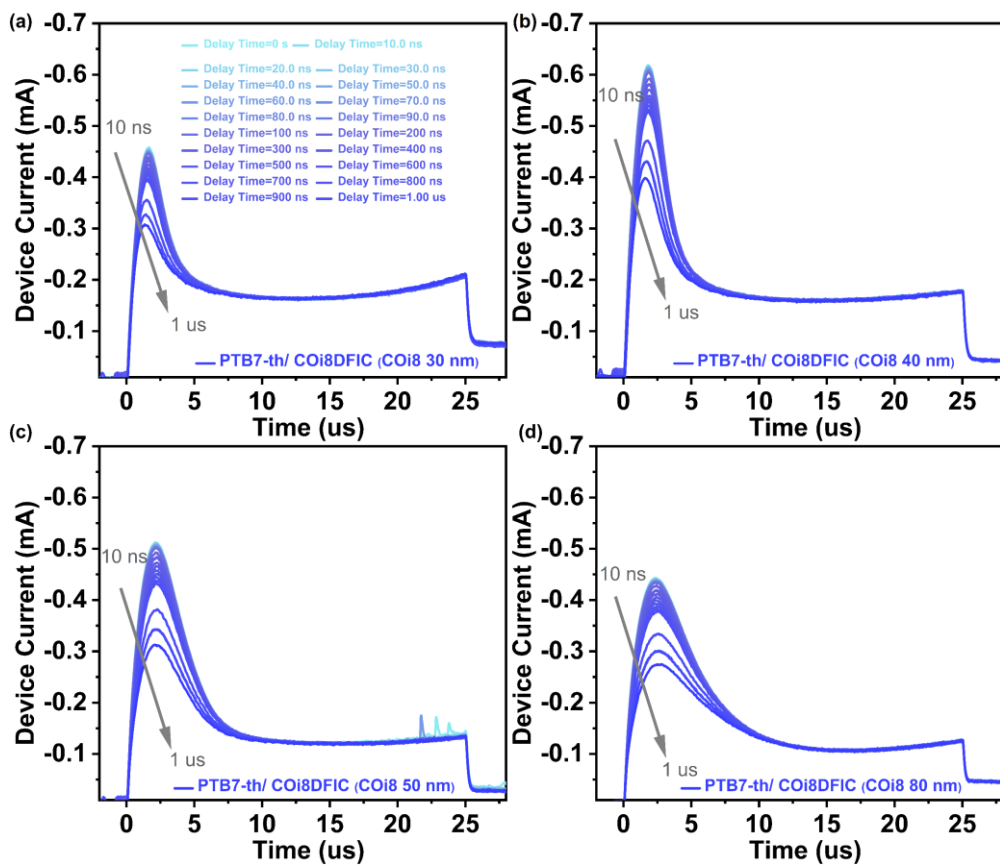


Figure S8. (a-d) Photo-CELIV measurements on the optimized PTB7-Th/COi8DFIC bilayer organic solar cells.

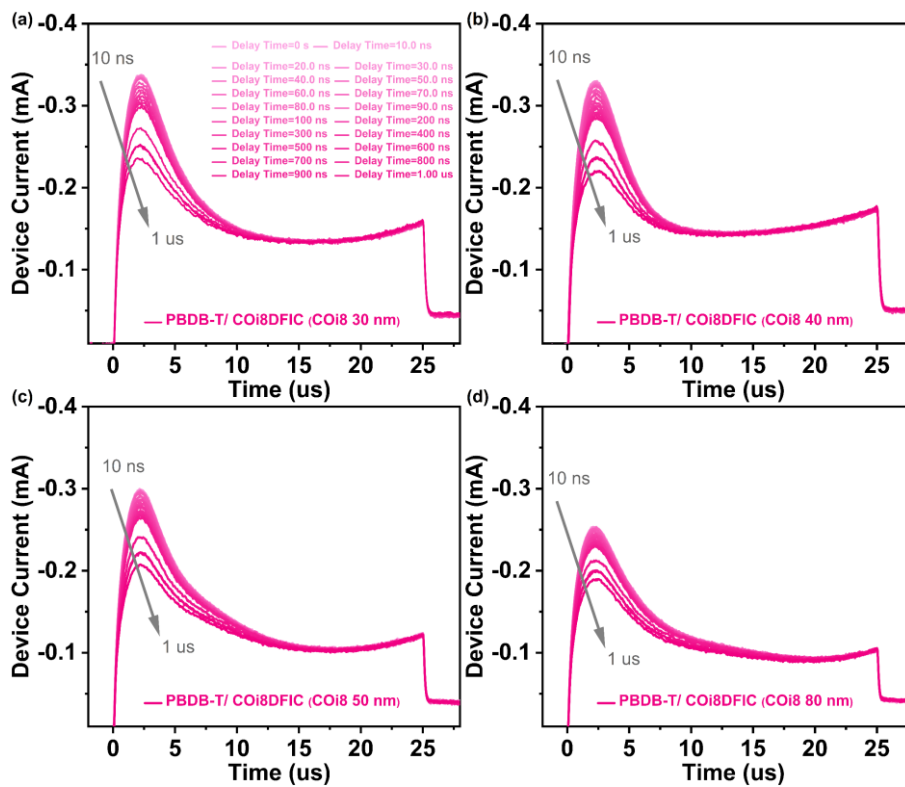


Figure S9. (a-d) Photo-CELIV measurements on the optimized PBDB-T/COi8-DFIC bilayer organic solar cells.

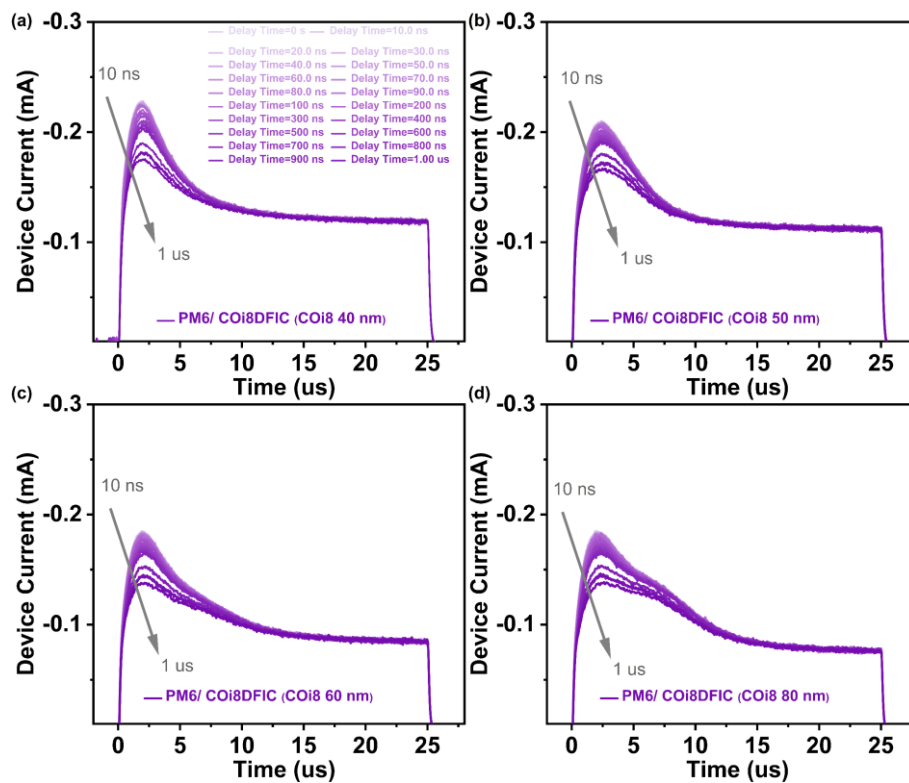


Figure S10. (a-d) Photo-CELIV measurements on the optimized PBDB-T-2F/COi8-DFIC bilayer organic solar cells.

Table S8. Dispersive bimolecular recombination fitting parameters. n_0 is the initial charge density, τ_b is the recombination lifetime, γ is the dispersion parameter, β is the bimolecular recombination rate at 10 ns.

Acceptor	Active Layer	β ($10^{-12} \text{ cm}^{-3} \text{ s}^{-1}$)	n_0 (cm^{-3})	γ	τ_b ($10^{-5} \mu\text{s}$)
8mg/ml	PTB7-Th/COI8DFIC	1.75	8.38	0.75	4.07
10mg/ml	PTB7-Th/COI8DFIC	1.74	6.39	0.85	1.84
12mg/ml	PTB7-Th/COI8DFIC	1.81	6.04	0.92	1.53
14mg/ml	PTB7-Th/COI8DFIC	2.16	5.34	0.90	1.82
6mg/ml	PBDB-T/COI8DFIC	1.71	7.61	0.73	5.77
8mg/ml	PBDB-T/COI8DFIC	1.38	6.96	0.82	3.80
10mg/ml	PBDB-T/COI8DFIC	2.12	5.26	0.81	3.47
12mg/ml	PBDB-T/COI8DFIC	2.07	4.51	0.84	3.29
14mg/m	PBDB-T/COI8DFIC	1.8	3.37	0.93	2.64
8mg/ml	PBDB-T-2F/COI8DFIC	1.65	5.44	0.75	7.71
10mg/ml	PBDB-T-2F/COI8DFIC	1.79	4.59	0.69	16.80
12mg/ml	PBDB-T-2F/COI8DFIC	1.90	3.53	0.85	4.54
14mg/ml	PBDB-T-2F/COI8DFIC	2.61	3.22	0.78	6.33

References

- 1- Firdaus, Y.; Le Corre, V. M.; Karuthedath, S. et al. Long-range exciton diffusion in molecular non-fullerene acceptors. *Nat Commun* 2020, 11 (1), 5220.
- 2- Powell, R. C.; Soos, Z. G. Singlet exciton energy transfer in organic solids. *Journal of Luminescence* 1975, 11 (1), 1-45.
- 3- Cook, S.; Furube, A.; Katoh, R. et al. Estimate of singlet diffusion lengths in PCBM films by time-resolved emission studies. *Chemical Physics Letters* 2009, 478 (1), 33-36.
- 4- Cook, S.; Liyuan, H.; Furube, A. et al. Singlet Annihilation in Films of Regioregular Poly(3-hexylthiophene): Estimates for Singlet Diffusion Lengths and the Correlation between Singlet Annihilation Rates and Spectral Relaxation. *The Journal of Physical Chemistry C* 2010, 114 (24), 10962-10968. DOI: 10.1021/jp101340b.

- 5- (5) Chandrabose, S.; Chen, K.; Barker, A. J.; Sutton, J. J.; Prasad, S. K. K.; Zhu, J.; Zhou, J.; Gordon, K. C.; Xie, Z.; Zhan, X.; et al. High Exciton Diffusion Coefficients in Fused Ring Electron Acceptor Films. *Journal of the American Chemical Society* 2019, 141 (17), 6922-6929. DOI: 10.1021/jacs.8b12982.
- 6- Mozer, Attila J., et al. "Time-dependent mobility and recombination of the photoinduced charge carriers in conjugated polymer/fullerene bulk heterojunction solar cells." *Physical Review B—Condensed Matter and Materials Physics* 72.3 (2005): 035217.
- 7- Mozer, Attila J., et al. "Charge transport and recombination in bulk heterojunction solar cells studied by the photoinduced charge extraction in linearly increasing voltage technique." *Applied Physics Letters* 86.11 (2005).
- 8- Liu, Yang, et al. "Trap-limited bimolecular recombination in poly (3-hexylthiophene): Fullerene blend films." *Organic Electronics* 38 (2016): 8-14.